Article

Preparation of a Titania/X-Zeolite/Porous Glass Composite Photocatalyst Using Hydrothermal and Drop Coating Processes

Atsuo Yasumori [1,2,*], Sayaka Yanagida [1,2] and Jun Sawada [1]

[1] Department of Materials Science and Technology, Tokyo University of Science, 6-3-1 Niijuku, Katsushika-ku, Tokyo 125-8585, Japan; E-Mails: YANAGIDA.Sayaka@nims.go.jp (S.Y.); bb_is_my_life_tr@yahoo.co.jp (J.S.)

[2] Photocatalysis International Research Center, Research Institute for Science and Technology, Tokyo University of Science, 2641 Yamazaki, Noda-shi, Chiba 278-8510, Japan

* Author to whom correspondence should be addressed; E-Mail: yasumori@rs.noda.tus.ac.jp; Tel.: +81-3-5876-1717 (ext. 1820); Fax: +81-3-5876-1639.

Abstract: Combinations of TiO_2 photocatalysts and various adsorbents have been widely studied for the adsorption and photocatalytic decomposition of gaseous pollutants such as volatile organic compounds (VOCs). Herein, a TiO_2-zeolite-porous glass composite was prepared using melt-quenching and partial sintering, hydrothermal treatment, and drop coating for preparation of the porous glass support and X-zeolite and their combination with TiO_2, respectively. The obtained composite comprised anatase phase TiO_2, X-zeolite, and the porous glass support, which were combined at the micro to nanometer scales. The composite had a relatively high specific surface area of approximately 25 m^2/g and exhibited a good adsorption capacity for 2-propanol. These data indicated that utilization of this particular phase-separated glass as the support was appropriate for the formation of the bulk photocatalyst-adsorbent composite. Importantly, the photocatalytic decomposition of adsorbed 2-propanol proceeded under UV light irradiation. The 2-propanol was oxidized to acetone and then trapped by the X-zeolite rather than being released to the atmosphere. Consequently, it was demonstrated that the micrometer-scaled combination of TiO_2 and zeolite in the bulk form is very useful for achieving both the removal of gaseous organic pollutants and decreasing the emission of harmful intermediates.

1. Introduction

Various atmospheric pollutants in the environment continue to cause considerable problems. In particular, volatile organic compounds (VOCs) such as formaldehyde, acetaldehyde, acetone, 2-propanol, and toluene, released mainly from paints and adhesives used in building and construction materials, give rise to sick building syndrome. Titanium dioxide (TiO₂) photocatalysts are well known to decompose organic compounds under ultraviolet (UV) light irradiation via oxidation reactions, and therefore, have been widely studied and are practically employed in combination with "black lights", such as fluorescent lamps, UV lamps, and sunlight to remove indoor VOCs [1–9].

The concentration of VOCs in living spaces is typically very low at several tens of ppm (by volume and used hereafter) to less than 1 ppm [10]. Under such conditions, a TiO₂ photocatalyst in the form of a coating material has two main disadvantages. First, the decomposition rate is not sufficiently high for gaseous pollutants at very low concentrations in the atmosphere, because the photocatalytic reaction mediated by TiO₂ (or any other solid semiconductor photocatalyst) occurs at or very close to the surface, and the diffusion process for the gaseous pollutants from the atmosphere to the surface of the TiO₂ is rate limiting. Second, the removal of VOCs is not effective under weak intensity radiation or during the nighttime.

One potential solution for overcoming such disadvantages of TiO₂ is the combination of a TiO₂ photocatalyst with an appropriate adsorbent. In such a composite, the pollutants are first concentrated in the pores of the adsorbent, and then photocatalytic degradation of the adsorbed or desorbed pollutants proceeds on the TiO₂ or in the pores due to the generation of oxygen radicals following light irradiation. Because the advantages of combining TiO₂ with an adsorbent are also observed for the degradation of dilute concentrations of pollutants in waste water, various adsorbents have been combined with TiO₂ for the rapid removal of low levels of pollutants in the environment [11]. For example, studies have been reported on the combination of TiO₂ photocatalysts with ceramic supports [12–16], porous glasses and glass fiber [17–21], activated carbon [22–26] and graphene [27–30], silica gel [31–35] and other mesoporous materials [36–40].

Zeolites are another important category of effective adsorbents that have been combined with TiO₂. Natural zeolite is an aluminosilicate mineral with micro pores. Various synthetic zeolites have been prepared with controllable pore sizes and surface properties and used as molecular sieves for the adsorption of molecules of particular sizes and polarities [41]. In addition, there are many studies of combinations of TiO₂ photocatalysts and zeolites for photochemical and photocatalytic science and applications [42,43]. For, example, studies have been reported on the adsorption and photocatalytic degradation of various organic pollutants [44–50] and nitrogen oxides (NOₓ) [51,52]. Among the synthesized zeolites, X- and Y-zeolites, which have faujasite (FAU) structure, are well known to have large pores (0.74 nm in diameter) due to their super cage structures and the ability to adsorb relatively large organic molecules [53]. Notably, the adsorption properties of those FAU-type zeolites are influenced by their

compositions, and particularly the Si/Al ratio. The number of Na^+ (or other alkaline or alkaline earth metal) ions accompanying the $[AlO_4]^-$ tetrahedra on the surface of X-zeolite is relatively high because of its low Si/Al ratio (Si/Al $\approx$ 1.25) compared to that of other FAU-type zeolites, such as Y-zeolite (Si/Al $\approx$ 2.3) [53]. Because cations on the surfaces of zeolite pores exhibit strong electrostatic interactions with molecules having dipole or quadrupole moments, X-zeolite can adsorb molecules, such as H_2O and lower alcohols. Therefore, in the present study, X-zeolite with its high ability for the adsorption of polar VOCs was selected as the adsorbent for the model polar VOC pollutant 2-propanol.

For preparation of a composite comprising TiO_2 and X-zeolite, three important points were considered. (1) It is necessary for the X-zeolite to be adjacent to the TiO_2 to ensure that photo-generated oxygen radicals diffuse and attack the VOCs adsorbed in the X-zeolite before they are deactivated [54,55]; (2) TiO_2 and the X-zeolite should be co-loaded on appropriate supports to enable easy handling in practical applications [56]; (3) A transparent support for the TiO_2 and X-zeolite is required to allow passage of near-UV light for photoexcitation of the TiO_2. Previous studies mentioned above could achieve the first point that the zeolite was adjacent to the TiO_2 by use of mainly commercial particulate zeolite and appropriate synthesis procedures of TiO_2 fine particles. However, for the practical application, the above points (2) and (3) are essential. In addition, the support should also be porous to provide a highly dispersive condition of zeolite which can result in a large adsorption and reaction area. Therefore, porous silicate glass was selected because of its high specific surface area, transparency in the visible and UV range, and relatively high chemical durability, and zeolite was directly synthesized on the glass support. The disk-shaped silicate glass supports were prepared via the partial sintering of silicate glass frits comprising Na_2O-B_2O_3-CaO-ZrO_2-Al_2O_3-SiO_2 with ratios in the immiscibility region to achieve phase separation [57]. The porous glass was formed during subsequent hydrothermal treatment, which was used for the synthesis of the X-zeolite on the glass support. This process was expected to make the zeolite combine with the porous support much rigidly. The TiO_2 was then coated on the X-zeolite on the glass support by dropping a titanium alkoxide solution into the zeolite-porous glass composites. The crystalline phases and microstructures of the obtained TiO_2-coated zeolite-porous glass composites were characterized and their ability to adsorb and photocatalytically decompose 2-propanol was examined.

2. Results and Discussion

2.1. Crystalline Phases of the Composites

The XRD patterns of the partially sintered glass and composite samples are shown in Figure 1. The partially sintered glass exhibited only a halo pattern in the diffraction pattern (Figure 1a,b), indicating that the glass was not crystallized during the sintering process. The diffraction pattern of the zeolite-porous glass composite (Figure 1c) contained diffraction peaks for the X-zeolite of a FAU structure, while that for the TiO_2-coated composite sample (Figure 1d) exhibited the diffraction peak for anatase TiO_2 in addition to those for the X-zeolite, although the intensities of the latter peaks were slightly decreased. These results indicated that the X-zeolite precipitated following hydrothermal treatment and remained in the composite following the TiO_2 coating process.
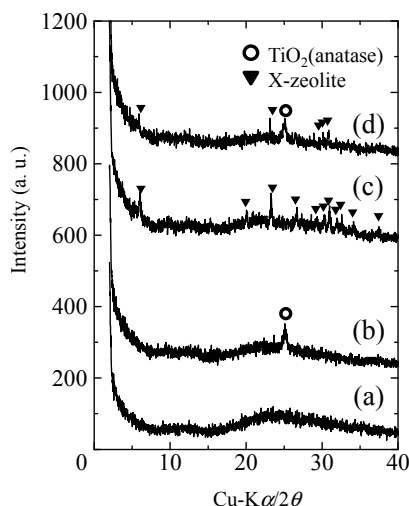
Figure 1. XRD patterns of the prepared samples: (a) partially sintered glass; (b) TiO$_2$-coated partially sintered glass; (c) zeolite-porous glass composite; and (d) TiO$_2$-coated zeolite-porous glass composite.

2.2. Micro Textures of the Composites

The micro textures of the TiO$_2$-coated partially sintered glass, the zeolite-porous glass composite, and the TiO$_2$-coated composite were observed via FE-SEM, and the results are shown in Figures 2–4, respectively. The TiO$_2$-coated partially sintered glass disk comprised glass particles with diameters of 100–200 μm (Figure 2a), which were similar to those of the raw glass frit particles. Sufficient spaces remained through which 2-propanol gas could diffuse to the interior of the disk. In addition, many small cracks were observed at the interfaces between the glass particles due to precipitation of the thick TiO$_2$ layer (Figure 2b). Interestingly, the zeolite-porous glass composite had a similar texture to that of the partially sintered glass on a macroscopic level, as can be seen in Figure 3a. However, in the microstructure near the surface that was directly exposed to the solution during hydrothermal treatment, many cubic precipitates were formed (Figure 3b), which were assigned to the X-zeolite based on their cubic shape [58] and the results of the XRD analysis. Micro pores formed by the selective etching of the phase separation texture during the hydrothermal treatment were also detected on the glass grains, as can be seen in Figure 3c. Finally, a thick TiO$_2$ layer covered the surface of the micro structure in the coated composite, but the texture of the sample was not changed significantly, as can be seen in Figure 4a–c. Figure 4d shows the coated X-zeolite as an example.
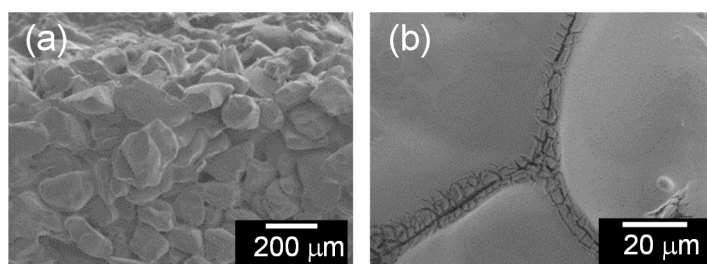
Figure 2. FE-SEM images of the TiO$_2$-coated partially sintered glass with (**a**) low and (**b**) high magnification.
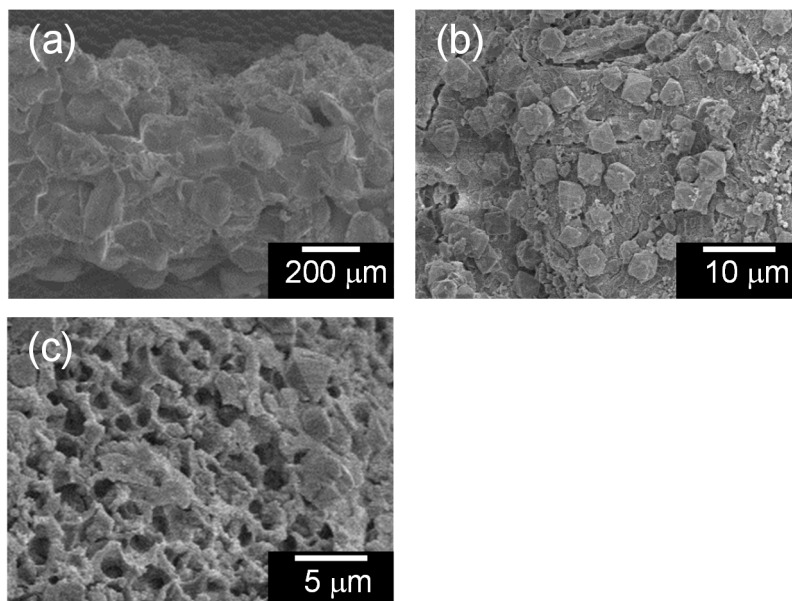
Figure 3. FE-SEM images of the zeolite-porous glass composite: (**a**) low magnification image; (**b**) precipitated zeolite particles; and (**c**) micro pores formed on the glass surface.
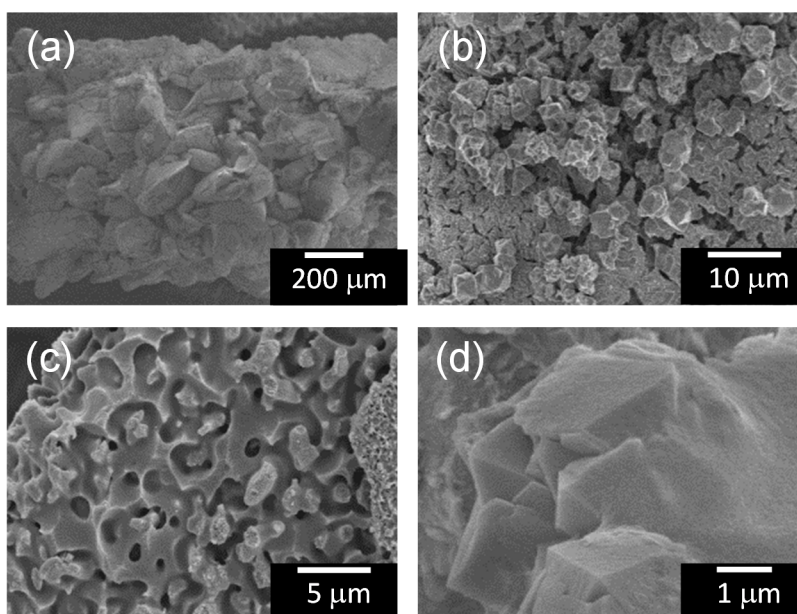
Figure 4. FE-SEM images of the TiO$_2$-coated zeolite-porous glass composite: (**a**) low magnification image; (**b**) precipitated zeolite particles; (**c**) micro pores formed on the glass surface; and (**d**) TiO$_2$ coating layer on the zeolite.

2.3. Adsorption Characteristics of the Composites

The adsorption and desorption isotherms of the zeolite-porous glass composite before and after TiO$_2$ coating are shown in Figure 5. Both samples exhibited definite hysteresis in the high relative pressure region, and these isotherms corresponded to type IV isotherms as classified by International Union of Pure and Applied Chemistry (IUPAC) [59]. Typical FAU type zeolites exhibit type II isotherms with little or no adsorption and hysteresis in the same region [59,60]. In contrast, type IV isotherms are

typically observed in silica gel or mesoporous silica [59]. Therefore, these isotherms indicated that the adsorption behavior of the composite could be attributed to the micropores of the zeolite and the mesopores of the porous glass in the low and the high relative pressure regions, respectively. Not surprisingly, the adsorption volume of the TiO2 coated sample was significantly decreased compared to that of the non-coated composite in the high relative pressure region. The multipoint Brunauer–Emmett–Teller (BET) specific surface area (Sg) of the zeolite-porous glass composite was approximately 30 m^2/g or approximately 4% that of a commercial X-zeolite (approximately 780 m^2/g, F9, Tosoh Co., Tokyo, Japan). After TiO2 coating, the samples retained a high Sg of approximately 25 m^2/g. These results indicated that the deposited TiO2 prevented the N2 gas from being adsorbed in the mesopores of the porous glass but allowed the gas to be adsorbed in the micropores of X-zeolite, and thus the combination of a TiO2 photocatalyst and X-zeolite adsorbent in a composite was successfully achieved. The Sg of the TiO2-coated partially sintered glass was less than the detection limit of the measurement system, suggesting that the coated TiO2 layer did not contribute to the adsorption of 2-propanol or acetone as an intermediate oxidative product of 2-propanol.
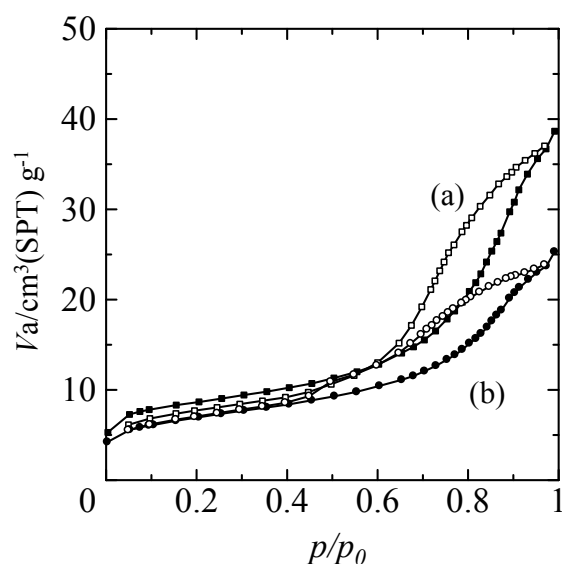
Figure 5. Adsorption and desorption isotherms of the zeolite-porous glass composite- (a) before and (b) after TiO2 coating.

Next, the adsorption of 2-propanol by the prepared composites was examined. The changes in the concentration of 2-propanol in the glass container with time under dark conditions are shown in Figure 6 for the TiO2-coated glass and the TiO2 coated zeolite-porous glass composite. The TiO2-coated glass adsorbed approximately 15% of the 2-propanol within the first 10 min, but then the concentration changed little up to 60 min. In contrast, the TiO2-coated zeolite-porous glass composite adsorbed most of the 2-propanol within 10 min because it had a much higher specific surface area than the TiO2-coated glass due to the presence of the X-zeolite.
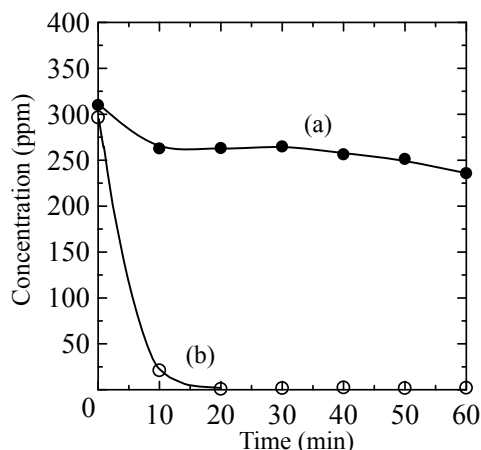
Figure 6. Change in the concentration of 2-propanol due to adsorption by the (a) TiO$_2$-coated partially sintered glass and (b) TiO$_2$-coated zeolite-porous glass composite.

2.4. Photocatalytic Properties of the Composites

The process of photocatalytic oxidation of 2-propanol has been well studied [54,61,62]. The reaction process is simply represented in Equations (1) and (2). Acetone is an intermediate product that is generated during the photocatalytic oxidative decomposition of 2-propanol:

$$C_3H_7OH + 1/2O_2 \rightarrow CH_3COCH_3 + H_2O \tag{1}$$

$$CH_3COCH_3 + 4O_2 \rightarrow 3CO_2 + 3H_2O \tag{2}$$
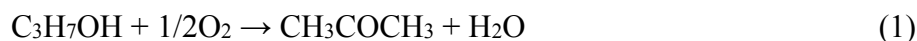
After adsorption of 2-propanol for 60 min, the samples were exposed to UV light irradiation, and the concentrations of 2-propanol, acetone, and CO$_2$ were determined by gas chromatography. The changes in the concentrations of these gaseous species during UV light irradiation are shown in Figure 7a,b for the TiO$_2$-coated partially sintered glass and the TiO$_2$-coated zeolite-porous glass composite, respectively. The concentration of CO$_2$ is presented as an increase over the initial concentration (ΔCO$_2$) as indicated by the values of the coordinates on the right vertical axis.
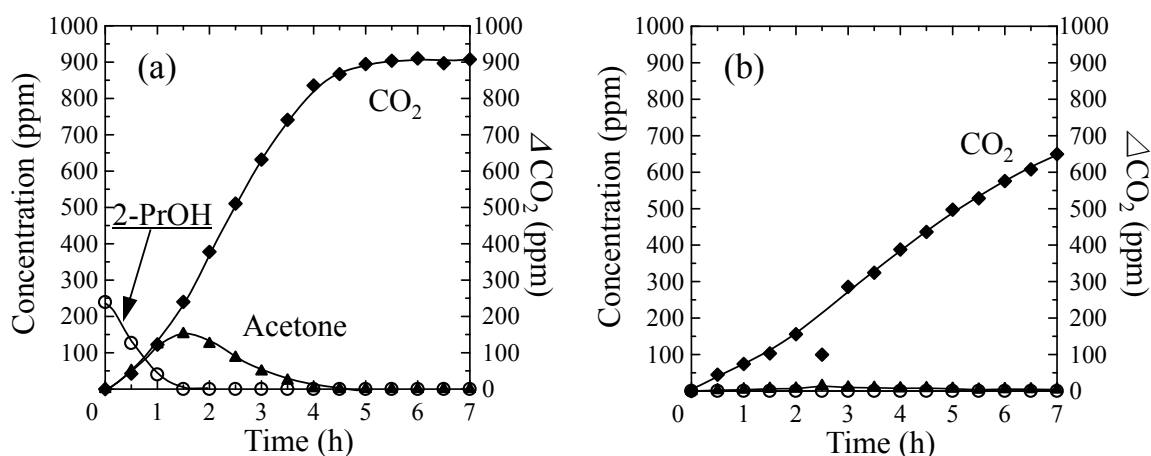
Figure 7. Changes in the concentrations of 2-propanol (open circles), acetone (filled triangles), and ΔCO$_2$ (filled diamonds, right axis) for the (**a**) TiO$_2$-coated partially sintered glass and (**b**) TiO$_2$-coated zeolite-porous glass composite.

In Figure 7a, the concentration of the residual 2-propanol gradually decreased and fell below the detection limit for the partially sintered TiO_2-coated glass after 1.5 h of UV light irradiation, while the concentration of acetone gradually increased to a maximum at 1.5 h, and then gradually decreased and fell below the detection limit after 4 h. The ΔCO_2 value also gradually increased to approximately 900 ppm and became saturated after approximately 5 h. This saturated value of approximately 900 ppm corresponded to the theoretical ΔCO_2 value expected for the complete conversion of 300 ppm of initial 2-propanol to H_2O and CO_2 via oxidation and decomposition as described in Equations (1) and (2).

With the TiO_2-coated partially sintered glass, a decrease in residual 2-propanol occurred simultaneously with an increase in the acetone and CO_2 concentrations, indicating that the 2-propanol was photocatalytically oxidized to acetone, a portion of which was immediately oxidized to CO_2 (Equations (1) and (2)), and a portion of which was released to the atmosphere. This behavior can be attributed to the lower adsorption capacity of the TiO_2-coated partially sintered glass.

In contrast, no desorption of 2-propanol to the atmosphere was detected for the TiO_2-coated zeolite-porous glass composite as shown in Figure 7b, and only a slight amount of acetone was observed. In addition, the ΔCO_2 value increased linearly with the UV light irradiation time. However, the generation rate for CO_2 was lower than that for the TiO_2-coated partially sintered glass, and the ΔCO_2 value was limited to approximately 650 ppm after 7 h. Considering the adsorption properties of X-zeolite as described in the introduction, the adsorption of 2-propanol and acetone on the X-zeolite in the present composite proceeded due to the electrostatic interactions between the Na^+ or K^+ ions on the surface of the X-zeolite and the 2-propanol and acetone. On the other hand, the adsorption of 2-propanol by the porous glass is considered to occur via hydrogen bonding, because Si-OH groups are likely to be present on the surface of the porous glass following hydrothermal treatment. However, based on the results of the FE-SEM analyses of the TiO_2-coated samples (Figures 2 and 4) and the decrease in the adsorption volume in the high relative pressure region (Figure 5), it is considered that the quantity of Si-OH groups decreased due to the subsequent repeated heat treatments at 400 °C and 500 °C necessary for fabrication of the TiO_2 coating and thick TiO_2 layer, respectively. Therefore, it can be concluded that the X-zeolite in the composite was the main adsorbent for the 2-propanol.

The schematic of the structure of the TiO_2-coated zeolite-porous glass composite are illustrated in Figure 8a,b in order to show its behaviors of adsorption and photocatalytic oxidation of 2-propanol and acetone, respectively. Even though CO_2 is not a polar molecule, it has a quadrupole moment and can thus also be adsorbed on X-zeolites via electrostatic interactions [63]. The adsorption behavior of the X-zeolite for 2-propanol, acetone, and CO_2 resulted in the slow generation rate of CO_2 from the zeolite-porous glass composite. In other words, although the X-zeolite strongly adsorbed 2-propanol and acetone, a certain amount of the CO_2 generated during irradiation with UV light was also adsorbed as shown in Figure 8b. These results suggest that the 2-propanol and acetone that desorbed from the X-zeolite (and the porous glass) were immediately oxidized by the TiO_2, which was adjacent to the X-zeolite. Alternatively, the 2-propanol and acetone adsorbed in the X-zeolite may have been attacked by oxygen radicals generated on the TiO_2 following irradiation with UV light. This oxidation process is possible to occur because the photocatalytic oxidation of 2-propanol sufficiently proceeded in the mechanically mixed zeolite and TiO_2 powder system [55], and in our composite system, the diffusion distance was enough short for the radicals generated from TiO_2 to reach the molecules adsorbed in the neighboring X-zeolite. Consequently, the TiO_2-coated zeolite-porous glass composite could sufficiently remove 2-propanol by

the adsorption and the photocatalytic oxidation and also it could suppress the release of acetone to the atmosphere during the photocatalytic decomposition process owing to its high adsorption capacity.
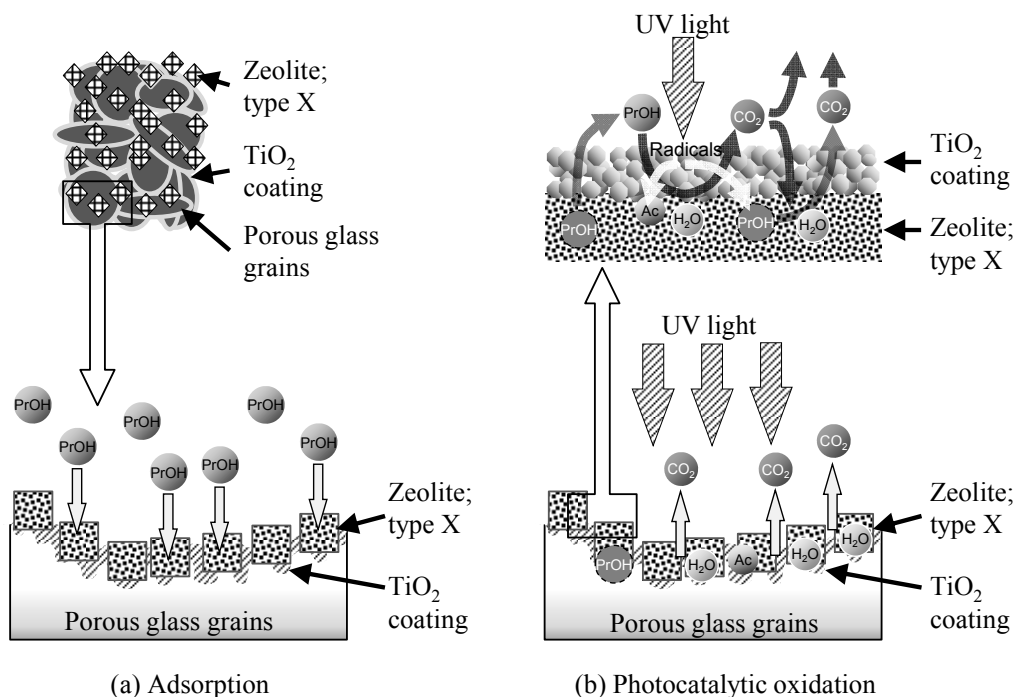
Figure 8. Schematic of (**a**) adsorption and (**b**) photocatalytic oxidation process by the TiO$_2$-coated zeolite-porous glass composite.

3. Experimental Section

3.1. Preparation of Partially Sintered Glass Supports

Porous silicate glass prepared using the phase separation phenomenon of oxide glasses was selected as the support. The sodium borosilicate glass system is considered to have a metastable immiscibility region and to separate into SiO$_2$-rich and Na$_2$O-B$_2$O$_3$ rich phases following appropriate thermal treatment above the glass transition temperature. In addition, SiO$_2$-rich porous glass can be obtained from such phase separated glasses with spinodal decomposition compositions upon further thermal treatment and subsequent selective leaching of the Na$_2$O-B$_2$O$_3$ rich phase [64]. Such a porous glass has been utilized as the support for TiO$_2$ photocatalysts [17,18]. However, for the synthesis of zeolites, it is necessary to use a hydrothermal treatment process in highly concentrated alkaline solution. Because typical SiO$_2$-rich glass has poor chemical resistance to alkaline solutions, it was necessary to use the mother glass, which has high durability in alkaline solutions, for synthesis of the glass-zeolite composite. Yazawa *et al.* reported that the Na$_2$O-B$_2$O$_3$-CaO-ZrO$_2$-Al$_2$O$_3$-SiO$_2$ glass system has a metastable immiscibility region, and the porous glass obtained from this system exhibited high durability in alkaline solutions [57]. Based on these results, a glass batch composition for the mother glass of 5.7Na$_2$O-9.2CaO-2.3Al$_2$O$_3$-3.2ZrO$_2$-22.7B$_2$O$_3$-56.9SiO$_2$ (mol %) was used in the present study.

Reagent-grade Na$_2$CO$_3$, H$_3$BO$_3$, SiO$_2$, CaCO$_3$, ZrO$_2$, and Al$_2$O$_3$ (Wako Pure Chemical, Osaka, Japan) were used for glass preparation without further purification. The glass batch was prepared by mixing the weighed raw materials and melting the mixture in an alumina crucible at 1500 °C for 1 h in air. The melt

was then quenched and immediately heat-treated at 750 °C for 12 h to allow phase separation to occur. Next, the partially sintered glass support was prepared by first grinding the annealed, heat-treated (phase separated) glass into 106–150 μm diameter particles and then forming the particles into a rod-like shape. The rod was sintered at 700 °C for 1 h, and then disk shapes were cut, each with a diameter of approximately 11 mm, a thickness of 1 mm, and a weight of 0.1 g.

3.2. Synthesis of the Zeolite on the Partially Sintered Glass Support

To form micro pores on the partially sintered glass disks, hydrothermal treatment was used to simultaneously etch the phase separated glass particles that formed the disk and synthesize the zeolite.

FAU type zeolites are well known to be synthesized by use of a mixed NaOH-KOH solution [65]. Precise preparation conditions of X-zeolite on the phase separated glass were determined based on the results of the preliminary experiments and were described as followings. Two partially sintered glass disks, one on top of the other, were placed in an aqueous solution containing NaOH (3 mol/L, 25 mL) and KOH (4 mol/L, 5 mL). Next, silica gel (0.4 g) and $NaAlO_2$ (0.4 g), both purchased from Wako Pure Chemical and used without further purification, were added as the silica and alumina sources, respectively. The sample was tightly closed in a Teflon container (diameter: 35 mm; height: 55 cm in inner dimension; volume: approximately 50 mL) and was maintained at 75 °C for 24 h with stirring at 500 rpm. The hydrothermally treated sample was then washed with distilled water until the pH of the rinse water was approximately 8 and finally dried at 60 °C for 24 h.

3.3. TiO$_2$ Coating of the Samples

TiO_2 thin films were coated on the zeolite-glass composite and partially sintered glass using titanium diisopropoxide bis(acetylacetonate) $[(CH_3)_2CHO]_2Ti(C_5H_7O_2)_2$; TPA, Aldrich, St. Louis, MO, USA) as the TiO_2 source. A 2-propanol solution of TPA (1 mass% Ti) was stirred at approximately 2 °C for 1 h. Next, 200 μL of the TPA solution was dropped into the sample, dried at room temperature for 5 min, and subsequently heated at 400 °C for 10 min. This dropping and subsequent drying/heating cycle was repeated 6 times. Finally, the samples were heated at 500 °C for 2 h.

3.4. Characterizations of the Samples

The crystalline phases precipitated in the samples were examined using X-ray diffraction (XRD) analysis (LabX XRD-6100, Shimadzu, Kyoto, Japan) with a Cu-K$_\alpha$ radiation source. The micro textures of the surfaces and the cross sections of the samples were observed via field emission scanning electron microscopy (FE-SEM; S-4200, Hitachi, Tokyo, Japan) after platinum sputter coating. The adsorption and desorption isotherms and multipoint BET specific surface areas (Sg) of the samples were determined using the nitrogen adsorption technique (BELSORP-mini II, Nippon Bell, Osaka, Japan). The samples were heated at 200 °C for 24 h in a vacuum prior to measurement.

3.5. Gas Adsorption Ability and Photocatalytic Activity of the Samples

A calibrated gas generator (Permeater PD-1B, Gastech, Kanagawa, Japan) and dried air were used to produce air-diluted 2-propanol gas (approximately 300 ppm). A glass container (diameter: 4 cm; height:

6 cm; volume: approximately 65 mL) was placed in a glove bag filled with the air-diluted 2-propanol gas, and then the container filled with the same 2-propanol gas, immediately sealed and kept in the dark at 20 °C. The concentration of 2-propanol was determined using a gas chromatograph (GC, GC-8A, Shimadzu) with a thermal conductivity detector (TCD), a porous polymer beads column (Sunpak-A, 2 m, 160 °C, Shinwa Chemical, Kyoto, Japan), and a He carrier gas (20 mL/min). The gas in the sealed container was sampled (1 mL) every 10 min for 60 min using a micro syringe. After determination of the gas adsorption ability, the glass bottle was irradiation with UV light from a black light lamp (FL15BLB, peak wavelength = 0.30 mW/cm^2 at 365 nm). The concentrations of 2-propanol, acetone, and CO_2 in the glass container were determined every 30 min for 7 h using the same GC procedure.

4. Conclusions

A TiO_2-zeolite-porous glass composite was prepared using melt-quenching for the glass preparation, hydrothermal treatment for the synthesis of the X-zeolite, and drop coating for deposition of the TiO_2 thin film. The obtained composite comprised anatase phase TiO_2, X-zeolite, and the porous glass, which were combined at the micro to nanometer scale. Synthesis of the X-zeolite on the porous glass support was possible because a glass with high resistance to alkaline solutions was used. In addition, the TiO_2 and X-zeolite were solidified and formed into a disk shape with a relatively high specific surface area, and importantly, the TiO_2 as the photocatalyst was adjacent to the X-zeolite as the adsorbent. Furthermore, the X-zeolite in the composite was very effective for the adsorption of polar molecules, such as 2-propanol as a model pollutant and acetone and its oxidized intermediate. The suppression of the release of acetone due to the presence of the X-zeolite suggested that the combined use of TiO_2 and an adequate adsorbent is very useful for decreasing the emission of harmful intermediates generated during photocatalytic oxidative decomposition. Finally, the phase separated glass used as the support for the loading of the zeolite and TiO_2 made it possible to prepare a bulk photocatalyst-adsorbent composite with superior adsorption and photo degradation properties for 2-propanol, and it was considered to be a good candidate for a composite of photocatalyst and adsorbent for the practical applications of the removal of gaseous organic pollutants.

Author Contributions

A.Y. designed and organized the study; J.S. and S.Y. performed the experiments; J.S., S.Y., and A.Y. analyzed the data; S.Y. and A.Y. wrote the paper.

Conflicts of Interest

References

1. Peral, J.; Ollis, D.F. Heterogeneous photocatalytic oxidation of gas-phase organics for air purification Acetone, 1-butanol, butyraldehyde, formaldehyde, and *m*-xylene oxidation. *J. Catal.* **1992**, *136*, 554–565.
2. Fox, M.A.; Dulay, M.T. Heterogeneous photocatalysis. *Chem. Rev.* **1993**, *93*, 341–357.

3. Hoffmann, M.R.; Martin, S.T.; Choi, W.; Bahnemann, D.W. Environmental Applications of Semiconductor Photocatalysis. *Chem. Rev.* **1995**, *95*, 69–96.

4. Fujishima, A.; Rao, T.N.; Tryk, D.A. Titanium dioxide photocatalysis. *J. Photchem. Photobiol. C Photochem. Rev.* **2000**, *1*, 1–21.

5. Zhao, J.; Yang, X. Photocatalytic oxidation for indoor air purification: A literature review. *Build. Environ.* **2003**, *38*, 645–654.

6. Hashimoto, K.; Irie, H.; Fujishima, A. TiO$_2$ Photocatalysis: A Historical Overview and Future Prospects. *Jpn. J. Appl. Phys.* **2005**, *44*, 8269–8285.

7. Mo, J.; Zhang, Y.; Xu, Q.; Lamson, J.J.; Zhao, R. Photocatalytic purification of volatile organic compounds in indoor air: A literature review. *Atmos. Environ.* **2009**, *43*, 2229–2246.

8. Chen, H.; Nanayakkara, C.E.; Grassian, V.H. Titanium Dioxide Photocatalysis in Atmospheric Chemistry. *Chem. Rev.* **2012**, *112*, 5919–5948.

9. Yu, C.W.F.; Kim, J.T. Photocatalytic Oxidation for Maintenance of Indoor Environmental Quality. *Indoor Built Environ.* **2013**, *22*, 39–51.

10. Chapter 4: Summary of the guidelines. In *Air Quality Guidelines for Europe*, 2nd ed.; WHO Regional Office for Europe, WHO Regional Publications, European Series: Copenhagen, Demark, 2000; pp. 32–33.

11. Shaham-Waldmann, N.; Paz, Y. Modified Photocatalysts. In *Photocatalysis and Water Purification*; Pichat, P., Ed.; Wiley-VCH: Weinheim, Germany, 2013; pp. 107–111.

12. Kato, K. Photocatalytic Property of TiO$_2$ Anchored on Porous Alumina Ceramic Support by the Alkoxide Method. *J. Ceram. Soc. Jpn.* **1993**, *101*, 245–249.

13. Sauer, M.L.; Ollis, D.F. Acetone Oxidation in a Photocatalytic Monolith Reactor. *J. Catal.* **1994**, *149*, 81–91.

14. Obee, T.N.; Brown, R.T. TiO$_2$ Photocatalysis for Indoor Air Applications Effects of Humidity and Trace Contaminant Levels on the Oxidation Rates of Formaldehyde, Toluene, and 1,3-Butadiene. *Environ. Sci. Technol.* **1995**, *29*, 1223–1231.

15. Yasumori, A.; Ishizu, K.; Hayashi, S.; Okada, K. Preparation of a TiO$_2$ based multiple layer thin film photocatalyst. *J. Mater. Chem.* **1998**, *8*, 2521–2524.

16. Yasumori, A.; Shinoda, H.; Kameshima, Y.; Hayashi, S.; Okada, K. Photocatalytic and photoelectrochemical propertiesof TiO$_2$-based multiple layer thin film prepared by sol–gel and reactive-sputtering methods. *J. Mater. Chem.* **2001**, *11*, 1253–1257.

17. Anpo, M.; Aikawa, N.; Kubokawa, Y. Photoluminescence and photocatalytic activity of highly dispersed titanium oxide anchored onto porous Vycor glass. *J. Phys. Chem.* **1985**, *89*, 5017–5021.

18. Yamashita, H.; Honda, M.; Harada, M.; Ichihashi, Y.; Anpo, M.; Hirao, T.; Itoh, N.; Iwamoto, N. Preparation of Titanium Oxide Photocatalysts Anchored on Porous Silica Glass by a Metal Ion-Implantation Method. *J. Phys. Chem. B* **1998**, *102*, 10707–10711.

19. Ao, C.H.; Lee, S.C.; Yu, J.C. Photocatalyst TiO$_2$ supported on glass fiber for indoor air purification effect of NO on the photodegradation of CO and NO$_2$. *J. Photochem. Photobiol. A Chem.* **2003**, *156*, 171–177.

20. Ho, W.H.; Yu, J.C.; Yu, J. Photocatalytic TiO$_2$/Glass Nanoflake Array Films. *Langmuir* **2005**, *21*, 3486–3492.

21. Machida, F.; Daiko, Y.; Mineshige, A.; Kobune, M.; Toyoda, N.; Yamada, I.; Yazawa, T. Structures and Photocatalytic Properties of Crystalline Titanium Oxide-Dispersed Nanoporous Glass-Ceramics. *J. Am. Ceram. Soc*. **2010**, *93*, 461–464.

22. Takeda, N.; Torimoto, T.; Sampath, S.; Kuwabata, S.; Yoneyama, H. Effect of Inert Supports for Titanium Dioxide Loading on Enhancement of Photodecomposition Rate of Gaseous Propionaldehyde. *J. Phys. Chem*. **1995**, *99*, 9986–9991.

23. Torimoto, T.; Okawa, Y.; Takeda, N.; Yoneyama, H. Effect of Activated Carbon Content in TiO_2-loaded Activated Carbon on Photodegradation Behaviors of Dichloromethane. *J. Photochem. Photobiol. A Chem*. **1997**, *103*, 153–157.

24. Huang, B.; Saka, S. Photocatalytic activity of TiO_2 crystallite-activated carbon composites prepared in supercritical isopropanol for the decomposition of formaldehyde. *J. Wood Sci*. **2003**, *49*, 79–85.

25. Ao, C.H.; Lee, S.C. Combination effect of activated carbon with TiO_2 for the photodegradation of binary pollutants at typical indoor air level. *J. Photochem. Photobiol. A Chem*. **2004**, *161*, 131–140.

26. Ao, C.H.; Lee, S.C. Indoor air purification by photocatalyst TiO_2 immobilized on an activated carbon filter installed in an air cleaner. *Chem. Eng. Sci*. **2005**, *60*, 103–109.

27. Kamat, P.V. Graphene-Based Nanoarchitectures. Anchoring Semiconductor and Metal Nanoparticles on a Two-Dimensional Carbon Support. *J. Phys. Chem. Lett*. **2010**, *1*, 520–527.

28. Zhang, H.; Lv, X.; Li, Y.; Wang, Y.; Li, J. P25-Graphene Composite as a High Performance Photocatalyst. *ACS Nano* **2010**, *4*, 380–386.

29. Zhang, Y.; Tang, Z.; Fu, X.; Xu, Y. TiO_2−Graphene Nanocomposites for Gas-Phase Photocatalytic Degradation of Volatile Aromatic Pollutant: Is TiO_2−Graphene Truly Different from Other TiO_2−Carbon Composite Materials. *ACS Nano* **2010**, *4*, 7303–7314.

30. Kamegawa, T.; Yamahana, D.; Yamashita, H. Graphene Coating of TiO_2 Nanoparticles Loaded on Mesoporous Silica for Enhancement of Photocatalytic Activity. *J. Phys. Chem. C* **2011**, *114*, 15049–15053.

31. Domen, K.; Sakata, Y.; Kudo, A.; Maruya, K.; Onishi, T. The Photocatalytic Activity of a Platinized Titanium Dioxide Catalyst Supported over Silica. *Bull. Chem. Soc. Jpn*. **1988**, *61*, 359–362.

32. Yasumori, A.; Yamazaki, K.; Shibata, S.; Yamane, M. Preparation of TiO_2 Fine Particles Supported on Silica Gel as Photocatalyst. *J. Ceram. Soc. Jpn*. **1994**, *102*, 702–707.

33. Anderson, C.; Bard, A.J. An Improved Photocatalyst of TiO_2/SiO_2 Prepared by a Sol-Gel Synthesis. *J. Phys. Chem*. **1995**, *99*, 9882–9885.

34. Ding, Z.; Hu, X.; Lu, G.Q.; Yue, P.; Greenfield, P.F. Novel Silica Gel Supported TiO2 Photocatalyst Synthesized by CVD Method. *Langmuir* **2000**, *16*, 6216–6222.

35. Ismail, A.A.; Ibrahim, I.A.; Ahmed, M.S.; Mohamed, R.M.; El-Shall, H. Sol–gel synthesis of titania–silica photocatalyst for cyanide photodegradation. *J. Photochem. Photobiol. A Chem*. **2004**, *163*, 445–451.

36. Yu, J.C.; Wang, X.; Fu, X. Pore-Wall Chemistry and Photocatalytic Activity of Mesoporous Titania Molecular Sieve Films. *Chem. Mater*. **2004**, *16*, 1523–1530.

37. Li, H.; Bian, Z.; Zhu, J.; Huo, Y.; Li, H.; Lu, Y. Mesoporous Au-TiO_2 Nanocomposites with Enhanced Photocatalytic Activity. *J. Am. Chem. Soc*. **2007**, *129*, 4538–4539.

38. Tan, L.K.; Kumar, M.K.; An, W.W.; Gao, H. Transparent, Well-Aligned TiO_2 Nanotube Arrays with Controllable Dimensions on Glass Substrates for Photocatalytic Applications. *Appl. Mater. Interfaces* **2010**, *2*, 498–503.

39. Chu, S.; Inoue, S.; Wada, K.; Li, D.; Haneda, H.; Awatsu, S. Highly Porous (TiO_2-SiO_2-TeO_2)/Al_2O_3/TiO_2 Composite Nanostructures on Glass with Enhanced Photocatalysis Fabricated by Anodization and Sol-Gel Process. *J. Phys. Chem. B* **2003**, *107*, 6586–6589.

40. Qian, X.F.; Kamegawa, T.; Mori, K.; Li, H.X.; Yamashita, H. Calcium Phosphate Coatings Incorporated in Mesoporous TiO_2/SBA-15 by a Facile Inner-pore Sol-gel Process toward Enhanced Adsorption-photocatalysis Performances. *J. Phys. Chem. C* **2013**, *117*, 19544–19551.

41. Sircar, S.; Myers, A.L. 22 Gas Separation by Zeolites. Part V Applications. In *Handbook of Zeolite Science and Technology*; Auerbach, S.M., Carrado, K.A., Dutta, P.K., Eds.; CRC Press: New York, NY, USA, 2003; pp. 1063–1104.

42. Corma, A.; Garcia, H. Zeolite-based photocatalysts. *Chem. Commun.* **2004**, 1443–1459, doi:10.1039/B400147H.

43. Kuwahara, Y.; Yamashita, H. Efficient photocatalytic degradation of organics diluted in water and air using TiO_2 designed with zeolites and mesoporous silica materials. *J. Mater. Chem.* **2011**, *21*, 2407–2416.

44. Sampath, S.; Uchida, H.; Yoneyama, H. Photocatalytic Degradation of Gaseous Pyridine over Zeolite-Supported Titanium Dioxide. *J. Catal.* **1994**, *149*, 189–194.

45. Torimoto, T.; Ito, S.; Kuwabata, S.; Yoneyama, H. Effects of Adsorbents Used as Supports for Titanium Dioxide Loading on Photocatalytic Degradation of Propyzamide. *Environ. Sci. Technol.* **1996**, *30*, 1275–1281.

46. Xu, Y.; Langford, C.H. Photoactivity of Titanium Dioxide Supported on MCM41, Zeolite X, and Zeolite Y. *J. Phys. Chem. B* **1997**, *101*, 3115–3121.

47. Ichiura, H.; Kitaoka, T.; Tanaka, H. Preparation of composite TiO_2-zeolite sheets using a papermaking technique and their application to environmental improvement Part I Removal of acetaldehyde with and without UV irradiation. *J. Mater. Sci.* **2002**, *37*, 2937–2941.

48. Takeuchi, M.; Kimura, T.; Hidaka, M.; Rakhmawaty, D.; Anpo, M. Photocatalytic oxidation of acetaldehyde with oxygen on TiO_2/ZSM-5 photocatalyst: Effect of hydrophobicity of zeolites. *J. Catal.* **2007**, *246*, 235–240.

49. Donphai, W.; Kamegawa, T.; Careonpanich, M.; Nueangnoraj, K.; Mishihara, H.; Kyotani, T.; Yamashita, H. Photocatalytic performance of TiO_2–zeolite templated carbon composites in organic contaminant degradation. *Phys. Chem. Chem. Phys.* **2014**, *16*, 25004–25007.

50. Kamegawa, T.; Ishiguro, Y.; Kido, R.; Yamashita, H. Design of Composite Photocatalyst of TiO_2 and Y-Zeolite for Degradation of 2-Propanol in the Gas Phase under UV and Visible Light Irradiation. *Molecules* **2014**, *19*, 16477–16488.

51. Ichiura, H.; Kitaoka, T.; Tanaka, H. Preparation of composite TiO_2-zeolite sheets using a papermaking technique and their application to environmental improvement, Part II Effect of zeolite coexisting in the composite sheet on NO_x removal. *J. Mater. Sci.* **2003**, *38*, 1611–1615.

52. Jan, Y.; Lin, L.; Karthik, M.; Bai, H. Titanium Dioxide/Zeolite Catalytic Adsorbent for the Removal of NO and Acetone Vapors. *J. Air Waste Manag. Assoc.* **2009**, *59*, 1186–1193.

53. Lobo, R.F. Introduction to the Structural Chemistry of Zeolites. Part II Synthesis and Structure. In *Handbook of Zeolite Science and Technology*; Auerbach, S.M., Carrado, K.A., Dutta, P.K., Eds.; CRC Press: New York, NY, USA, 2003; pp. 65–89.

54. Ohko, Y.; Kashimoto, K.; Fujishima, A. Kinetics of Photocatalytic Reactions under Extremely Low-Intensity UV Illumination on Titanium Dioxide Thin Films. *J. Phys. Chem. A* **1997**, *101*, 8057–8062.

55. Yamaguchi, K.; Inumaru, K.; Oumi, Y.; Sano, T.; Yamanaka, S. Photocatalytic decomposition of 2-propanol in air by mechanical mixtures of TiO_2 crystalline particles and silicalite adsorbent: The complete conversion of organic molecules strongly adsorbed within zeolitic channels. *Microporous Mesoporous Mater*. **2009**, *117*, 350–355.

56. Robert, D.; Keller, V.; Keller, N. Immobilization of a Semiconductor Photocatalyst on Solid Suppors: Methods, Materials, and Applications. In *Photocatalysis and Water Purification*; Pichat, P., Ed.; Wiley-VCH: Weinheim, Germany, 2013; pp. 145–178.

57. Yazawa, T.; Tanaka, H.; Eguchi, K.; Yokoyama, S. Novel alkali-resistance porous glass prepared from a mother glass based on the SiO_2-B_2O_3-RO-ZrO_2 (R=Mg, Ca, Sr, Ba and Zn) system. *J. Mater. Sci*. **1994**, *29*, 3433–3440.

58. Subotić, B.; Bronić, J. 5 Theoretical and Practical Aspects of Zeolite Crystal Growth. Part II Synthesis and Structure. In *Handbook of Zeolite Science and Technology*; Auerbach, S.M., Carrado, K.A., Dutta, P.K., Eds.; CRC Press: New York, NY, USA, 2003; pp. 129–203.

59. Sing, K.S.W.; Everett, D.H.; Haul, R.A.W.; Moscou, L.; Pierotti, R.A.; Rouquĕrol, J.; Siemieniewska, T. Reporting Physisorption Data for Gas/Solid Systems with Special Reference to the Determination of Surface Area and Porosity. *Pure Appl. Chem*. **1986**, *57*, 603–619.

60. Yang, Y.; Burke, N.; Zhang, J.; Huang, S.; Lim, S.; Zhu, Y. Influence of charge compensating cations on propane adsorption in X zeolites: Experimental measurement and mathematical modeling. *RSC Adv*. **2014**, *4*, 7279–7287.

61. Bickley, R.I.; Munuera, G.; Stone, F.S. Photoadsorption and Photocatalysis at Rutile Surfaces II. Photocatalytic Oxidation of Isopropanol. *J. Catal*. **1973**, *31*, 398–407.

62. Raillard, C.; Héquet, V.; Cloirec, P.L.; Legrand, J. Kinetic study of ketones photocatalytic oxidation in gas phase using TiO_2-containing paper: Effect of water vapor. *J. Photochem. Photobiol. A Chem*. **2004**, *163*, 425–431.

63. Cheung, O.; Hedin, N. Zeolites and related sorbents with narrow pores for CO_2 separation from flue gas. *RSC Adv*. **2014**, *4*, 14480–14494.

64. Doremus, R.H. 4 Phase Separation. Part One Formation and Structure of Glasses. In *Glass Science*; John Wiley & Sons: New York, NY, USA, 1973; pp. 44–73.

65. Kűhl, G.H. Crystallization of low-silica faujasite (SiO_2/Al_2O_3~2.0). *Zeolites* **1987**, *7*, 451–457.

Sample Availability: Melt-quenched glass samples are available from the authors.